

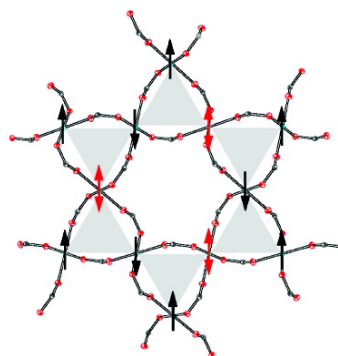
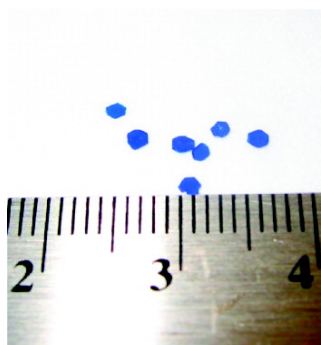
Communication

**A Structurally Perfect  $S = 1$  Metal–Organic Hybrid Kagomé Antiferromagnet**

Emily A. Nytko, Joel S. Helton, Peter Müller, and Daniel G. Nocera

*J. Am. Chem. Soc.*, **2008**, 130 (10), 2922–2923 • DOI: 10.1021/ja709991u

Downloaded from <http://pubs.acs.org> on February 8, 2009



**More About This Article**

Additional resources and features associated with this article are available within the HTML version:

- Supporting Information
- Links to the 2 articles that cite this article, as of the time of this article download
- Access to high resolution figures
- Links to articles and content related to this article
- Copyright permission to reproduce figures and/or text from this article

[View the Full Text HTML](#)

## A Structurally Perfect $S = 1/2$ Metal–Organic Hybrid Kagomé Antiferromagnet

Emily A. Nytko,<sup>†</sup> Joel S. Helton,<sup>‡</sup> Peter Müller,<sup>†</sup> and Daniel G. Nocera<sup>\*,†</sup>

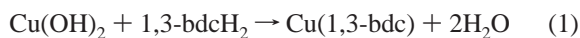
Departments of Chemistry and Physics, Massachusetts Institute of Technology, 77 Massachusetts Avenue, Cambridge, Massachusetts 02139-4307

Received November 5, 2007; E-mail: nocera@mit.edu

Geometric spin frustration occurs when the structural arrangement of spins precludes the simultaneous satisfaction of all nearest-neighbor interactions.<sup>1,2</sup> The corner-sharing equilateral triangles of a kagomé lattice present an excellent construct on which to study spin frustration; spin liquid physics can result when the kagomé lattice features  $S = 1/2$  spins on lattice vertices.<sup>3–5</sup> However, compounds bearing the kagomé structural motif are rare,<sup>6–10</sup> and exceptionally so when an organic moiety is a structural constituent of the kagomé triangles.<sup>11–14</sup> Previous studies of spin frustration on metal–organic hybrid kagomé compounds have been complicated by long exchange pathways,<sup>15,16</sup> triangulated<sup>17,18</sup> or interpenetrating structures,<sup>19</sup> and spin centers composed of dimers displaying intradimer exchange interactions.<sup>20–23</sup> There are some structurally distorted metal–organic hybrid kagomé with isolated metal ions (Co–Zn–Cd) on the vertices<sup>11</sup> and fewer structurally perfect systems (In, V, Zn);<sup>12–14</sup> none are composed of  $S = 1/2$  magnetic ions. We report herein the synthesis and magnetic characterization of the first structurally perfect metal–organic hybrid kagomé with a spin of  $S = 1/2$  on lattice vertices.

We recently employed a hydrothermal approach to prepare the first structurally perfect  $S = 1/2$  kagomé all-inorganic antiferromagnet, herbertsmithite  $\text{ZnCu}_3(\text{OH})_6\text{Cl}_2$ .<sup>9</sup> This remarkable material shows no long-range ordering to 50 mK,<sup>24</sup> despite having strongly antiferromagnetic nearest-neighbor superexchange, as evidenced by  $\Theta_{\text{CW}} = -314$  K. We have subsequently sought to generalize the  $S = 1/2$  kagomé lattice by discovering new systems that can be prepared in crystalline form.

Initial treatment of  $\text{Cu}(\text{OH})_2$  with isophthalic acid (1,3-bdcH<sub>2</sub>) under hydrothermal conditions led to the formation of a novel metal–organic hybrid kagomé,  $\text{Cu}(1,3\text{-bdc})$  (**1**), according to the condensation reaction below:



The product mixture also contains 1,3-bdcH<sub>2</sub> and a copper-containing ligand oxidation byproduct. (Ligand oxidation of 1,3-bdcH<sub>2</sub> in Cu(II)-containing solutions has been previously reported.<sup>25,26</sup>) To increase the solubility of 1,3-bdcH<sub>2</sub> and to buffer the reaction solution, imidazole was added to subsequent reactions. Additionally,  $\text{Cu}(\text{OH})\text{F}$  was included as a mineralizing agent to promote crystal formation. Large (up to 2 mm on an edge and 2.2 mg), dark blue hexagonal plates of **1** were separated from a product mixture containing starting materials and a copper-containing ligand oxidation byproduct,  $\text{C}_{32}\text{H}_{24}\text{Cu}_6\text{O}_{26}$  (**3**) (see Supporting Information, SI). **1** may contain an incidental guest water molecule upon structural analysis, so crystals of **1** were heated prior to magnetic measurements in order to remove the incidental solvent molecule (see SI). The purity of **1** was confirmed by similarities between simulated and experimental powder X-ray diffraction (pXRD) and

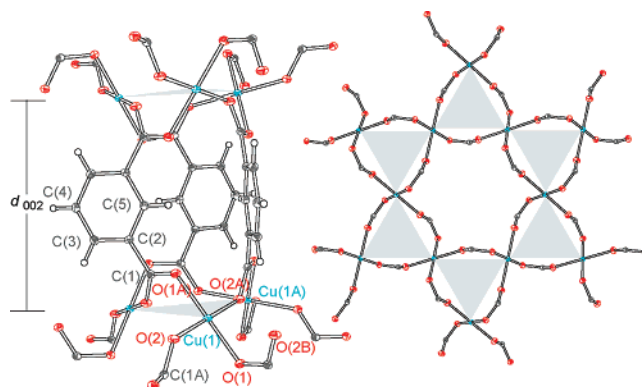


**Figure 1.** Crystal structure of **1**. Left: Interlayer coordination environment projected parallel to the crystallographic  $c$ -axis. Right: The organic–inorganic hybrid kagomé lattice, projected perpendicular to the  $c$ -axis. Phenyl ring atoms and guest water molecule have been omitted for clarity. Selected interatomic distances and angles: Cu(1)–O(1), 1.9265(9); Cu(1)–O(2), 1.9428(9); Cu(1A)···O(2B), 2.8396(9); Cu(1)–C(1A), 1.2685(15); O(2A)–C(1), 1.2689(14) Å; O(1)–Cu(1)–O(2), 92.14(4)°; O(2)–Cu(1)–O(1A), 87.86(4)°; Cu(1)–O(1)–C(1A), 115.67(8)°; Cu(1)–O(2A)–C(1), 132.42(8)°.

by elemental analysis (see SI, Figure S7). Solubility appears to play an important role in the formation of **1**, as related compounds  $\text{Cu}(\text{H}_2\text{O})(1,3\text{-bdc})\cdot\text{H}_2\text{O}$  and  $\text{Cu}_{24}(1,3\text{-bdc})_{24}(\text{DMF})_{14}(\text{H}_2\text{O})_{10}\cdot(\text{H}_2\text{O})_{10}(\text{DMF})_6(\text{C}_2\text{H}_5\text{OH})_6$  can be obtained from reactions with cupric acetate and cupric nitrate, respectively.<sup>27,28</sup>

The single-crystal X-ray structure of **1** is shown in Figure 1. Details of the structure solution and refinement are provided in the SI. The compound crystallizes in the hexagonal space group  $P6_3/m$ . The highly symmetric structure has only one-half of a crystallographically independent Cu(II) ion, which resides in a nearly square planar coordination environment with four monodentate carboxylate ligands. Each carboxylate group bridges two copper ions to form a kagomé lattice in the  $ab$  plane composed of  $\{\text{Cu}_3(\text{OCO})_3\}$  triangles. The in-plane Cu–Cu distance is 4.5541(2) Å (4.5528(3) Å for **2**,  $\text{Cu}(1,3\text{-bdc})\cdot 0.11 \text{H}_2\text{O}$ , the water-containing species), and the distance between the kagomé planes ( $d_{002}$ ) is 7.9716(3) Å (7.9775(6) Å for **2**). The layers stack in AA fashion. 1,3-bdc ligands serve to link the layers together into a three-dimensional metal–organic framework. The structure has hexagonal channels, with a solvent-accessible void of 45 Å<sup>3</sup> and a cross-channel Cu–Cu distance of 9.1081(2) Å (9.1056(3) Å for **2**). The guest water molecule residing in the center of this channel in the kagomé plane can be removed by heating the crystals to 240 °C without significant decomposition (see SI, Figure S2).

Fitting the high-temperature inverse susceptibility data (150–350 K) of a ground powder of **1** yields  $\Theta_{\text{CW}} = -33$  K, which suggests that the mean nearest-neighbor superexchange interaction is antiferromagnetic (see SI, Figure S3). The zero-field-cooled and field-cooled magnetic susceptibility of **1** versus temperature are shown in Figure 2a. A plot of  $\chi T$  vs  $T$  is provided in the SI, Figure

<sup>†</sup> Department of Chemistry.

<sup>‡</sup> Department of Physics.

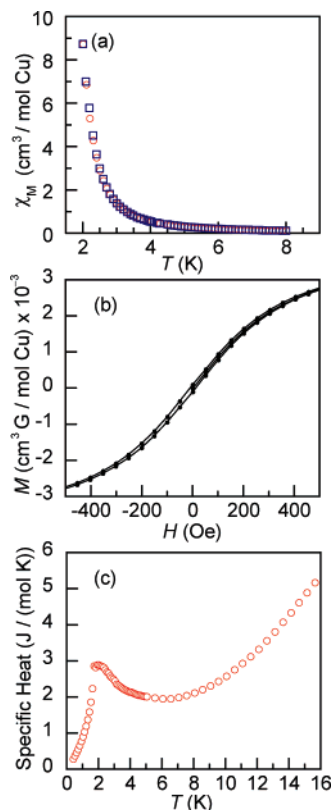


**Figure 2.** (a) Temperature dependence of  $\chi_M$  for a ground powder sample of **1** as measured at 100 Oe under zero-field-cooled (○) and field-cooled (□) conditions. Inset: Temperature dependence of  $\chi_M T$  for the same powder sample. (b) Field dependence of the magnetization per mole of Cu for **1**, measured at 2 K. The line is drawn to guide the eye. (c) Temperature dependence of the specific heat for a single crystal of **1** measured in zero field.

S4. Interestingly, both plots show an increase at low  $T$ , suggestive of the onset of a ferromagnetic ordering transition at the temperature limit of the SQUID susceptometer. Further evidence for a ferromagnetic ordering transition is provided by the magnetization versus field data measured at 2 K (Figure 2b) and the zero-field heat capacity versus temperature of a single crystal (Figure 2c). Figure 2b shows the small hysteresis loop indicative of a very soft ferromagnet with a coercive field of 10.5 Oe and a remanence of 95.8 emu Oe/mol Cu. Figure 2c shows a singularity in the heat capacity at 2 K, consistent with the onset of magnetic ordering at that temperature.

The foregoing magnetic data suggest a spin-frustrated behavior of **1**. Ramirez has provided a measure for spin frustration by defining  $f = |\Theta_{CW}|/T_c$ , with values of  $f > 10$  signifying a strong effect.<sup>1</sup> By this definition, **1** is spin frustrated, with a value of  $f = |-33 \text{ K}|/2 \text{ K} = 16.5$ . The in-plane superexchange between copper centers bridged by the 1,3-bdc linker in **1** is most likely antiferromagnetic. Copper centers bridged by monodentate carboxylates are typically coupled by antiferromagnetic superexchange interactions, as reported for paddlewheel complexes.<sup>29</sup> Model copper dimer systems with geometries similar to that of **1** suggest that the origin of the ferromagnetic behavior is derived from superexchange through the 1,3-bdc linker to Cu ions in different layers. In Cu dimer model complexes,<sup>30,31</sup> Cu coupling is ferromagnetic and small in magnitude along a seven-atom superexchange pathway. The same pathway connects Cu ions in different layers of **1**.

The organic–inorganic hybrid spin-frustrated material, **1**, is distinguished by its short three-atom bridge between Cu centers, thus giving rise to the shortest known metal–metal distance in any

metal–organic hybrid kagomé to date. The ability to obtain crystals of moderate size opens the way for magnetoanisotropy measurements and, with still larger crystal sizes, inelastic neutron scattering measurements. Owing to the  $S = 1/2$  spin on a kagomé lattice, the discovery of inorganic–organic hybrid materials such as **1** provides a venue for the exploration of quantum disordered ground states in two dimensions.

**Acknowledgment.** This work made use of the Shared Experimental Facilities supported by the MRSEC Program of the National Science Foundation under award number DMR 02-13282. We thank NSF for providing E.A.N. with a predoctoral fellowship, Mr. T. McClure and Dr. S. Chu for experimental assistance, and Drs. B. Bartlett, D. Villagrán, and D. Grohol and Profs. M. Shores and Y. S. Lee for helpful discussions.

**Supporting Information Available:** Complete synthetic protocol and characterization of  $\text{CuC}_8\text{H}_4\text{O}_4$ ; crystallographic tables and X-ray crystallographic information, in CIF format, for **1**–**3**. This material is available free of charge via the Internet at <http://pubs.acs.org>.

## References

- Ramirez, A. P. *Annu. Rev. Mater. Sci.* **1994**, *24*, 453–480.
- Greedan, J. E. *J. Mater. Chem.* **2001**, *11*, 37–53.
- Lhuillier, C.; Misguich, G. *Lect. Notes Phys.* **2002**, *595*, 161–190.
- Grohol, D.; Matan, K.; Cho, J. H.; Lee, S. H.; Lynn, J. W.; Nocera, D. G.; Lee, Y. S. *Nat. Mater.* **2005**, *4*, 323–328.
- Matan, K.; Grohol, D.; Nocera, D. G.; Yildirim, T.; Harris, A. B.; Lee, S. H.; Nagler, S. E.; Lee, Y. S. *Phys. Rev. Lett.* **2006**, *96*, 247201/1–4.
- Grohol, D.; Papoutsakis, D.; Nocera, D. G. *Phys. Rev. B* **2003**, *67*, 064401/1–13.
- Bartlett, B. M.; Nocera, D. G. *J. Am. Chem. Soc.* **2005**, *127*, 8985–8993.
- Nocera, D. G.; Bartlett, B. M.; Grohol, D.; Papoutsakis, D.; Shores, M. P. *Chem. Eur. J.* **2004**, *10*, 3850–3859.
- Shores, M. P.; Nytko, E. A.; Bartlett, B. M.; Nocera, D. G. *J. Am. Chem. Soc.* **2005**, *127*, 13462–13463.
- Behera, J. N.; Rao, C. N. R. *J. Am. Chem. Soc.* **2006**, *128*, 9334–9335.
- Russanov, E. B.; Ponomorova, V. V.; Stoeckli-Evans, H.; Fernandez-Ibañez, E.; Stoeckli, F.; Sieler, J.; Domasevitch, K. V. *Angew. Chem., Int. Ed.* **2003**, *42*, 2499–2501.
- Liu, Y.; Kravtsov, V. C.; Beauchamp, D. A.; Eubank, J. F.; Eddaoudi, M. *J. Am. Chem. Soc.* **2005**, *127*, 7266–7267.
- Barthelet, K.; Marrot, J.; Férey, G.; Riou, D. *Chem. Commun.* **2004**, 520–521.
- Chun, H.; Moon, J. *Inorg. Chem.* **2007**, *46*, 4371–4373.
- Liu, H.-K.; Sun, W.-Y.; Tang, W.-X.; Yamamoto, T.; Ueyama, N. *Inorg. Chem.* **1999**, *38*, 6313–6316.
- Narumi, Y.; Honda, Z.; Katsumata, K.; Domenge, J. C.; Sindzingre, P.; Lhuillier, C.; Matsuo, A.; Suga, K.; Kindo, K. *J. Magn. Magn. Mater.* **2004**, *272–276*, 878–879.
- Norman, R. E.; Rose, N. J.; Stenkamp, R. E. *J. Chem. Soc., Dalton Trans.* **1987**, 2905–2910.
- Mekata, M.; Abdulla, M.; Asano, T.; Kikuchi, H.; Goto, T.; Morishita, T.; Hori, H. *J. Magn. Magn. Mater.* **1998**, *177–181*, 731–732.
- Manson, J. L.; Ressouche, E.; Miller, J. S. *Inorg. Chem.* **2000**, *39*, 1135–1141.
- Moulton, B.; Lu, J.; Hajndl, R.; Hariharan, S.; Zaworotko, M. *J. Am. Chem. Soc.* **2002**, *124*, 2821–2824.
- Atwood, J. L. *Nat. Mater.* **2002**, *1*, 91–92.
- Furukawa, S.; Ohba, M.; Kitagawaa, S. *Chem. Commun.* **2005**, 865–867.
- Liu, B.; Li, Y.-Z.; Zheng, L.-M. *Inorg. Chem.* **2005**, *44*, 6921–6923.
- Helton, J. S.; Matan, K.; Shores, M. P.; Nytko, E. A.; Bartlett, B. M.; Yoshida, Y.; Takano, Y.; Qiu, Y.; Chung, J.-H.; Nocera, D. G.; Lee, Y. S. *Phys. Rev. Lett.* **2007**, *98*, 107204/1–4.
- Yang, S.-Y.; Long, L.-S.; Huang, R.-B.; Zheng, L.-S.; Ng, S. W. *Inorg. Chim. Acta* **2005**, *358*, 1882–1886.
- Jiang, Y.-Q.; Zhou, Z.-H.; Wei, Z.-B. *Chin. J. Struct. Chem.* **2005**, *4*, 457–461.
- Gao, L.; Zhao, B.; Li, G.; Shi, Z.; Feng, S. *Inorg. Chem. Commun.* **2003**, *6*, 1249–1251.
- Eddaoudi, M.; Kim, J.; Wachter, J. B.; Chae, H. K.; O’Keefe, M.; Yaghi, O. M. *J. Am. Chem. Soc.* **2001**, *123*, 4368–4369.
- Jotham, R. W. *J. Chem. Soc., Dalton Trans.* **1972**, 428–438.
- Cheng, P.; Yan, S.-P.; Xie, C.-Z.; Zhao, B.; Chen, X.-Y.; Liu, X.-W.; Li, C.-H.; Lia, D.-Z.; Jiang, Z.-H.; Wang, G.-L. *Eur. J. Inorg. Chem.* **2004**, 2369–2378.
- Shen, W.-Z.; Chen, X.-Y.; Cheng, P.; Yan, S.-P.; Zhai, B.; Liao, D.-Z.; Jiang, Z.-H. *Eur. J. Inorg. Chem.* **2005**, 2297–2305.

JA709991U